

Analysis of an eddy current brake for an actuator of a high-voltage direct current circuit breaker

Min-Seob Sim¹, Jong-Suk Ro¹ ✉

¹School of Electrical and Electronics Engineering, Chung-Ang University, Dong-jak, Seoul, Republic of Korea

✉ E-mail: jongsukro@gmail.com

ISSN 1751-8660

Received on 1st January 2019

Revised 14th May 2019

Accepted on 16th May 2019

E-First on 10th June 2019

doi: 10.1049/iet-epa.2019.0002

www.ietdl.org

Abstract: High-voltage direct current (HVDC) system is difficult to proliferate due to the absence of a useful brake for the HVDC circuit breaker. To overcome this problem, this study proposes a useful brake, termed as an Eddy current brake (EB). A time-consuming time step analysis using the finite element method (FEM) is required to analyse the EB. To address this problem, a rapid and accurate analysis method is proposed using the equivalent circuit model, equation of motion, and the Runge–Kutta method. This technique is termed as the EER method in this research. The characteristic of the EB is analysed by using the proposed EER method and the results are compared with those of the 2D FEM analysis. The usefulness of the proposed EER method with regard to accuracy and rapidness is confirmed via 2D FEM analysis.

1 Introduction

High-voltage direct current (HVDC) systems have many merits such as high efficiency and low cost of transmission, ease of connection between different electric power systems, and efficient linkage with a renewable energy source [1–4].

The HVDC systems, however, have difficulties in wide spreading despite its merits. One of the main reasons for that is due to the difficulty of development of HVDC circuit breaker (CB) to break a DC fault current [5–9]. This is because it is difficult to develop a proper high-speed actuator system for HVDC CBs. The main barrier against developing the high-speed actuator system is the damage caused by the bouncing of the mover of the actuator located at the end of the opening [10–13]. This damage results in serious problems such as failure to break the fault current, potentially causing damage to property and life as well as increased maintenance costs.

To solve this problem, diverse kinds of mechanisms for braking, such as a spring mechanism and an inverse magnetic force generation coil mechanism, have been proposed [14–17]. However, conventional mechanisms have serious problems regarding performance, cost, volume, and so on. Thus, no solution exists for the brake of the actuator for HVDC CBs.

This study fills the above-mentioned gap by proposing a useful brake, termed as Eddy current brake (EB). The proposed EB does not suffer from the problems that occur in the previously proposed mechanisms, and is compact, simple, stable, and inexpensive compared to the conventional brakes.

The dynamic characteristic of the EB is non-linear. Hence, a significantly time-consuming time step analysis using the finite element method (FEM) is required to analyse the EB. While designing the EB, numerous models need to be analysed by using time step analysis with the FEM and a trial-and-error method. In other words, the analysis and design of the EB entail significant time and cost. An equivalent circuit analysis method, an intuitive and rapid analysis method have been studied in [18]. However, the method proposed in [18] cannot be applied for the analysis of the proposed EB due to the difference of structure and working principle of the model. Different from the method proposed in [18], in the analysis of the proposed EB, the influences of a permanent magnet, the external mechanical force, the element segmentation, and others should be considered with the derivation of a proper equivalent circuit model and parameter values for the proposed EB.

To address this issue, a rapid and accurate analysis technique, which is a combination of the equivalent circuit model, equation of

motion, and the Runge–Kutta method, is proposed in this research. It is called the EER method for short. In this method, an equivalent circuit model of permanent magnet and analytical equations for the calculation of circuit constants for EB are derived. The usefulness of the proposed EB and EER method is validated by the JMAG commercial FEM tool, the accuracy of which has been verified.

2 Structure and working principle of the EB

2.1 Structure of the proposed EB

As shown in Fig. 1, the proposed EB is divided into two main parts: a fixed part and a moving part. The fixed part includes a urethane buffer, conductive copper, and a metal cylinder. These components do not move. The moving part includes a moving magnet and a shaft, which are connected to the actuator.

2.2 Working principle of the EB

The magnet moves in the axial direction due to the kinetic energy of the actuator and is guided through the shaft. Therefore, the amount of magnetic flux passing through the cylindrical surface perpendicular to the shaft axis varies with the change in the position of the permanent magnet. As per Faraday's law, an electromotive force opposite to the magnetic flux change is induced and an eddy current flows along the circumference of the conductive copper. A magnetic repulsive force is generated between the eddy current and the moving magnet and it acts as a braking force for the moving part.

When the moving part arrives at the end of the cylinder, the kinetic energy of the moving part may be retained. It is termed as residual kinetic energy. In this case, the urethane buffer absorbs the residual kinetic energy of the moving part and prevents mechanical damage to the device.

2.3 Merits of the EB

The proposed EB is superior to the conventional braking mechanisms regarding size, cost, stability, and durability when it is used as a brake of the HVDC CB. Specifically:

- The EB can decelerate the mover stably. It is low-cost and has a compact structure because it does not need any power source or control circuit and operates passively due to the movement of the mover.

- The EB can be applied as the brake of a high-speed HVDC CB because its braking force is proportional to the speed of the mover.
- The durability and stability of the EB are higher than that of conventional mechanical brakes because there is no mechanical connection needs to be applied to the mover to generate the braking force.
- After the completion of the opening, the CB must hold the mover to maintain the open state. The conventional brake springs maintain the force in the opposite direction of motion even after stopping the mover. Therefore, an additional holding force is required to prevent the mover from returning due to the spring force. However, the eddy currents of the EB disappear when the mover reaches the end position and the velocity decreases to zero. The EB is therefore structurally simple and significantly superior in terms of cost and volume.

3 Proposed EER method

As stated previously, the dynamic characteristic of the EB is non-linear. Therefore, a time step analysis is essential to analyse the EB. However, a time step analysis with the FEM entails considerable computation time. Hence, a rapid and accurate time step analysis method is proposed for the EB by using the equivalent circuit model, equation of motion, and the Runge–Kutta method.

3.1 Equivalent circuit model for the EB

Equivalent electrical circuit models for the moving magnet and conductive copper of the EB are derived to estimate the electromagnetic characteristics of the EB as follows.

3.1.1 Derivation of the equivalent circuit for the moving magnet: Since the permanent magnet is the same as an electromagnet with a constant magnetomotive force, it can be modelled as a constant current source, as shown in Fig. 2. The flux of the moving magnet is magnetically coupled to the eddy currents flowing through the conductive copper, and this property can be modelled as mutual inductances between the magnet and eddy currents, as demonstrated in Fig. 2. Briefly, the moving magnet can be modelled as an equivalent electric circuit composed of the constant current source and the inductor.

The value of the equivalent current of the permanent magnet can be calculated as follows [19]:

$$i_m = H_C \cdot L_{mag} \quad (1)$$

where H_C is the coercive force of the permanent magnet, and L_{mag} is the axial length of the permanent magnet.

3.1.2 Derivation of the equivalent circuit for the conductive copper: If conductive copper is considered as a group of annular elements divided along the axial direction, each element can be modelled as a resistor–inductor circuit, illustrated in Fig. 2. The resistance value along the circumferential direction of the copper element of Fig. 2 is the resistance value of the circuit. Magnetic coupling with the permanent magnet and other elements is modelled as mutual inductance, and that of the coupling to itself is modelled as self-inductance [18].

The flux linkage λ_i of the i th element of conductive copper is the sum of the flux linkage generated by the eddy currents and the permanent magnet. The time derivative of λ_i can be expressed as

$$\begin{aligned} \frac{d\lambda_i}{dt} &= \sum_{j=1}^n L_{ij} \frac{di_j}{dt} + \frac{dL_{im}}{dz} \cdot \frac{dz}{dt} i_m + L_{im} \frac{di_m}{dt} \\ &= \sum_{j=1}^n L_{ij} \frac{di_j}{dt} + \frac{dL_{im}}{dz} \cdot v \cdot i_m \end{aligned} \quad (2)$$

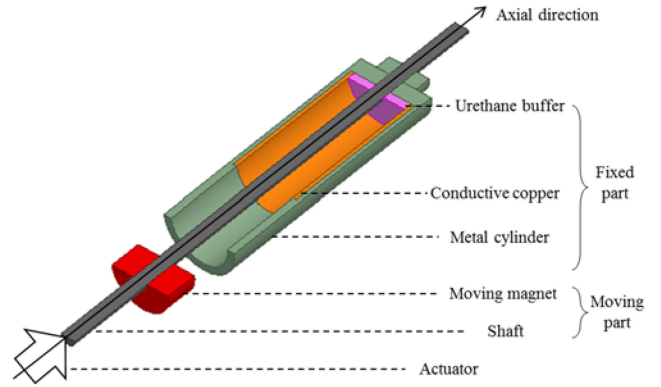


Fig. 1 Structure of the proposed EB for the HVDC CB

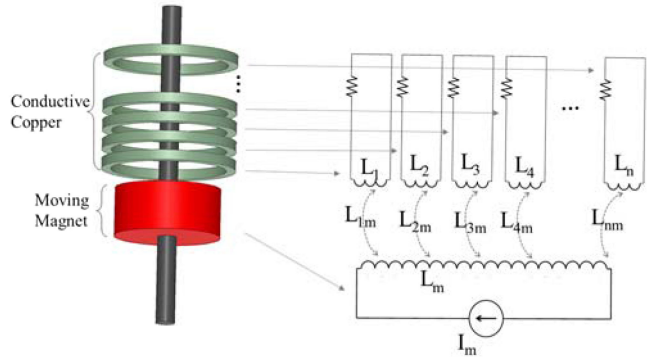


Fig. 2 Equivalent electric circuit for the EB

where L_{ij} is the mutual inductance between the i th and j th elements of conductive copper, L_{im} is the mutual inductance between the permanent magnet and the i th element, i_m is the equivalent current value of the permanent magnet, i_j is the current of the j th conductive copper element, v is the velocity of the moving magnet, and z is the axial distance.

According to Faraday's law, the time derivative of the flux linkage is equal to the voltage induced in the coil, which can be expressed by

$$\frac{d\lambda_i}{dt} = -V_{L_i} = -i_j R_i \quad (3)$$

where V_{L_i} is the voltage induced in the i th element, and R_i is the resistance of the i th element.

The differential equation of the eddy currents i_j with respect to time t can be derived as a matrix form from (2) and (3) using

$$\begin{pmatrix} L_{11} & L_{12} & \cdots & L_{1n} \\ L_{21} & L_{22} & \cdots & L_{2n} \\ \vdots & \vdots & \ddots & \vdots \\ L_{n1} & L_{n2} & \cdots & L_{nn} \end{pmatrix} \cdot \begin{pmatrix} i_1 \\ i_2 \\ \vdots \\ i_n \end{pmatrix} = \begin{pmatrix} -i_1 R_1 - v i_m \frac{dL_{1m}}{dz} \\ -i_2 R_2 - v i_m \frac{dL_{2m}}{dz} \\ \vdots \\ -i_n R_n - v i_m \frac{dL_{nm}}{dz} \end{pmatrix} \quad (4)$$

3.1.3 Calculation of the values of inductance and resistance: To solve (4), the values of inductance and resistance should be obtained.

The value of the i th self-inductance L_{ii} can be calculated by using Maxwell's approximate formula as follows [20]:

$$\begin{aligned} D_G &= 0.2235 (W_C + H_C) \\ L_{ii} &= \mu_0 R_C (\ln 8R_C / D_G \cdot (1 + 3D_G^2 / 16R_C^2) - (2 + D_G^2 / 16R_C^2)) \end{aligned} \quad (5)$$

where H_C is the axial length of conductive copper, W_C is the radial thickness of conductive copper, μ_0 is the permeability of vacuum, and R_C is the centre radius of conductive copper.

The value of mutual inductance L_{ij} between the i th and the j th copper elements can be calculated by using Rowland's second approximation as follows [20]:

$$L_{ij} = M_0 + \frac{1}{12} \left(H_C^2 \frac{dM_0}{dz^2} + W_C^2 \frac{dM_0}{dR_C^2} \right) \quad (6)$$

where M_0 is the mutual inductance between central turns of the i th and the j th copper elements.

The mutual inductance L_{im} between conductive copper element and permanent magnet can be calculated by using the formula of mutual inductance between coaxial circular filaments as follows [20]:

$$L_{im} = \frac{\mu_0 R_m R_C}{2} \int_0^{2\pi} \frac{\cos \theta}{\sqrt{d^2 + R_m^2 + R_C^2 - 2R_m R_C \cos \theta}} d\theta \quad (7)$$

where R_m is the radius of the equivalent current loop of permanent magnet and d is the axial distance between the equivalent current loop of permanent magnet and conductive copper element.

The derivative of L_{im} with respect to the axial displacement z can be calculated by differentiating L_{im} as follows:

$$\frac{dL_{im}}{dz} = \frac{\mu_0 R_m R_C}{2} \int_0^{2\pi} \frac{d \cos \theta}{(d^2 + R_m^2 + R_C^2 - 2R_m R_C \cos \theta)^{3/2}} d\theta \quad (8)$$

The resistance value R_i of the i th conductive copper element can be calculated as follows:

$$R_i = \rho_{\text{Copper}} \cdot \frac{\pi(R_{in} + R_{out})}{H_C W_C} \quad (9)$$

where ρ_{Copper} is a resistivity of copper, R_{in} is the inner radius of the conductive copper, and R_{out} is the outer radius of the conductive copper.

3.1.4 Determination of the number of conductive copper elements: The larger the number n of conductive copper elements, the more convergent and more accurate the analysis results. However, as n becomes larger, the size of the matrix becomes larger and the analysis time becomes longer. Therefore, the value of n , which makes the result, converged and minimises the analysis time should be obtained. When the aspect ratio of the conductive copper is about 1, the above is satisfied, and the value of n is calculated as follows:

$$n \cong \frac{H_{\text{Copper}}}{W_{\text{Copper}}} \quad (10)$$

where H_{Copper} is the axial height of conductive copper, and W_{Copper} is the radial thickness of conductive copper.

Conductive copper has the limitation of the effective radial thickness because there is an effective penetration depth of magnetic flux for the copper. Therefore, in a well-designed EB structure, it has the cylinder structure which has thin radial thickness with respect to the axial height. The density of induced eddy currents is almost uniform along the radial line within the range of W_{Copper} , so conductive copper does not need to be divided in the radial direction.

3.2 Formulation of the magnetic braking force

The magnetic force f_e on a moving magnet is equal to the value obtained by taking a negative value for the derivative of inner energy W_e of the EB with respect to the distance z , as derived by

$$f_e = - \frac{dW_e}{dz} = - \sum_{i=1}^n i_i \cdot i_m \cdot \frac{dL_{im}}{dz} \quad (11)$$

3.3 Derivation of equation of motion for the EB

The equation of motion for the calculation of position and velocity of the moving part of EB is induced by

$$\begin{pmatrix} 1 & 0 \\ 0 & 1 \end{pmatrix} \cdot \begin{pmatrix} \dot{z} \\ \dot{v} \end{pmatrix} = \begin{pmatrix} v \\ \frac{-f_e - f_f - f_g}{M} \end{pmatrix} \quad (12)$$

where f_f is the frictional force due to air resistance and surface friction, f_g is the gravitational force, and M is the mass of the moving part.

The frictional force f_f is calculated as the sum of the frictional force between shaft and fixed parts and the air resistance force due to the compressed air in the cylinder. And the equation of f_f is derived as follows:

$$f_f = \mu_s F_n + \frac{nRT}{((1 + \lambda) \cdot H_{\text{Copper}} - z)} \quad (13)$$

where μ_s is the coefficient of friction, F_n is the normal force on the friction surface, n is the amount of moles of the air in the cylinder, R is the gas constant of the air in the cylinder, T is the absolute temperature of the air in the cylinder, and λ is the compensation factor to prevent the divergence of the air resistance force into infinity at the position where z equals to H_{Copper} .

When λ is defined as the value between 0.02 and 0.05, it does not distort the original curve of the air resistance force and well prevent the divergence of the value at the end point.

3.4 Derivation of the governing equation for the motional and electrical characteristics of EB

By combining (4) and (12), the governing equation for the mechanical and electrical characteristics of the EB can be obtained as shown as follows:

$$\begin{pmatrix} L_{11} & L_{12} & \cdots & L_{1n} & 0 & 0 \\ L_{21} & L_{22} & \cdots & L_{2n} & 0 & 0 \\ \vdots & \vdots & \ddots & \vdots & \vdots & \vdots \\ L_{n1} & L_{n2} & \cdots & L_{nn} & 0 & 0 \\ 0 & 0 & \cdots & 0 & 1 & 0 \\ 0 & 0 & \cdots & 0 & 0 & 1 \end{pmatrix} \cdot \begin{pmatrix} i_1 \\ i_2 \\ \vdots \\ i_n \\ \dot{z} \\ \dot{v} \end{pmatrix} = \begin{pmatrix} -i_1 R_1 - v i_m \frac{dL_{1m}}{dz} \\ -i_2 R_2 - v i_m \frac{dL_{2m}}{dz} \\ \vdots \\ -i_n R_n - v i_m \frac{dL_{nm}}{dz} \\ v \\ \frac{-f_e - f_f - f_g}{M} \end{pmatrix} \quad (14)$$

By solving (14) using the Runge–Kutta method, the electrical and mechanical characteristics such as eddy currents, position, velocity, and acceleration of the EB can be analysed according to the time variation.

4 Data calculated using the EER method

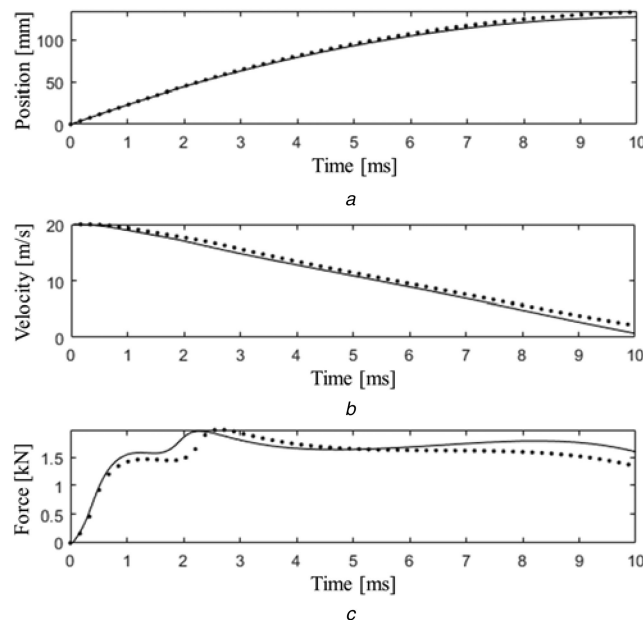
The operation of the EB is analysed by using the proposed EER method and comparing the results with those of the 2D FEM analysis using JMAG as follows:

4.1 Results calculated using the EER method

The characteristics of the proposed EB shown in Table 1 are calculated using the proposed EER method and 2D-FEM, as illustrated in Fig. 3. The figure confirms that the EB effectively damps the kinetic energy of the moving part within the requirements for the HVDC CB, such as the braking distance of 130 mm and the braking time of 10 ms.

Table 1 Specification of the proposed EB

Variable	Value
moving magnet height	40 mm
magnet material	Nd-Fe-B
cylinder's inner radius	40 mm
cylinder's outer radius	50 mm
mover mass	1 kg
initial velocity	20 m/s

**Fig. 3** Calculated characteristics of the EB using the EER method (straight line) and 2D-FEM (dotted line) (a) Position, (b) Velocity, (c) Force**Table 2** Comparison of braking time and distance calculated by EER method and 2D-FEM analysis

Magnet height, mm	EER method		2D FEM		Error rate	
	Braking distance, mm	Braking time, ms	Braking distance, mm	Braking time, ms	Braking distance, %	Braking time, %
25	181	14	198	15.4	-8.6	-9.1
30	164	13.8	173	13	-4.6	-6.1
35	146	11.1	152	11.6	-3.3	-2.6
40	130	10	133	10.6	-1.6	-4.1

Table 3 Comparison of computation time of the EER method with the computation time of 2D-FEM analysis

Magnet height, mm	Computation time		Computation time ratio (EER method:2D FEM)
	EER method, s	2D FEM, s	
25	15	2081	1:138.7
30	13	1618	1:124.5
35	12	1284	1:107
40	10	1090	1:109

Fig. 3 validates that the moving part of the HVDC CB decelerates dramatically because of the EB; the velocity of the moving part is significantly reduced before it arrives at the end of the opening. This reduces the mechanical damage to the mover and cylinder, increasing the reliability and life of the HVDC CB. These results prove that the EB is a useful brake for high-speed actuators such as those of the HVDC CB.

4.2 Comparison of the proposed EER method with results of 2D-FEM analysis

As shown in Table 2, the data calculated using the EER method match well with the 2D FEM results. The error rate is within the acceptable limit. Furthermore, the computation time as per the EER

method is significantly less than that of the 2D FEM, as shown in Table 3. Briefly, the usefulness of the proposed EER method with regard to accuracy and rapidness is confirmed.

5 Conclusion

The absence of a useful brake for the actuator of the HVDC CB has been widely recognised as a barrier against the widespread use of the HVDC system. This paper contributes to the literature by proposing and validating a useful brake (called the EB) for the HVDC CB.

The proposed EB can be used not only as a brake but also as an open-state holding structure. Therefore, the proposed EB is

remarkable in that it can dramatically reduce the cost and volume of the CB.

Analysis of the EB requires significant time when conducting a time step analysis with the FEM. Hence, it is noteworthy that this paper presented a rapid and accurate analysis method, called the EER method, to reduce the time and cost for the analysis and design of the EB and provide guidance for the design of electrical devices using eddy current and permanent magnets considering mechanical external forces.

Importantly, the proposed EB and EER technique can be applied to diverse kinds of electric machines, resulting in ripple effects in the research of electric machines.

6 Acknowledgments

This research was supported by the Chung-Ang University Graduate Research Scholarship in 2017 and by the Human Resources Development (No. 20184030202070) of the Korea Institute of Energy Technology Evaluation and Planning(KETEP) grant funded by the Korea government Ministry of Trade, Industry and Energy.

7 References

- [1] Garzon, R.D.: *High voltage circuit breakers design and applications* (Marcel Dekker, Inc., New York, NY, USA, 2011, 2nd edn.)
- [2] Bresesti, P., Kling, W.L., Hendriks, R.L., *et al.*: 'HVDC connection of offshore wind farms to the transmission system', *IEEE Trans. Energy Convers.*, 2007, **22**, (1), pp. 37–43
- [3] Franck, C.M.: 'HVDC circuit breakers – a review', *IEEE Trans. Power Deliv.*, 2011, **26**, (2), pp. 998–1007
- [4] Mitra, B., Chowdhury, B., Manjrekar, M.: 'HVDC transmission for access to off-shore renewable energy: a review of technology and fault detection techniques', *IET Renew. Power Gener.*, 2018, **12**, (13), pp. 1563–1571
- [5] Ragaller, K.: *Current interruption in high-voltage networks* (Springer, New York, NY, USA, 1978)
- [6] Park, S.H., Jang, H.J., Chong, J.K., *et al.*: 'Dynamic analysis of Thomson coil actuator for fast switch of HVDC circuit breaker'. 2015 3rd Int. Conf. Electric Power Equipment – Switching Technology ICEPE-ST 2015, Busan, Republic of Korea, 2015, pp. 425–430
- [7] Wu, Y., Wu, Y., Rong, M., *et al.*: 'A new Thomson coil actuator: principle and analysis', *IEEE Trans. Compon. Packag. Manuf. Technol.*, 2015, **5**, (11), pp. 1644–1655
- [8] Pei, X., Smith, A.C., Shuttleworth, R., *et al.*: 'Fast operating moving coil actuator for a vacuum interrupter', *IEEE Trans. Energy Convers.*, 2017, **32**, (3), pp. 931–940
- [9] Effah, F.B., Clare, J., Davidson, C., *et al.*: 'Hybrid HVDC circuit breaker with self-powered gate drives', *IET Power Electron.*, 2016, **9**, (2), pp. 228–236
- [10] Vilchis-Rodriguez, D.S., Shuttleworth, R., Barnes, M.: 'Finite element analysis and efficiency improvement of the Thomson coil actuator'. 8th IET Int. Conf. on Power Electronics, Machines and Drives (PEMD 2016), Glasgow, UK, 2016, p. pp. 6–6
- [11] Zhu, J., Men, B., Huang, Y., *et al.*: 'Closing performance of the Thomson-coil actuator for a 110 kV FMS'. 14th IET Int. Conf. on AC and DC Power Transmission, Chengdu, People's Republic of China, 2018, pp. 3–7
- [12] Gao, Y., Huang, Z., Wang, Y., *et al.*: 'Investigations on the safe stroke of mechanical HVDC vacuum circuit breaker'. 14th IET Int. Conf. on AC and DC Power Transmission, Chengdu, People's Republic of China, 2019, pp. 1–4
- [13] Shuttleworth, R., Smith, A.C., Barnes, M.: 'A comparison of damping techniques for the soft-stop of ultra-fast linear actuators for HVDC breaker applications'. PEMD, Liverpool, UK, April 2018, pp. 1–6
- [14] Peng, C., Mackey, L., Husain, I., *et al.*: 'Active damping of ultra-fast mechanical switches for hybrid AC and DC circuit breakers'. ECCE 2016 – IEEE Energy Conversion Congress Exposition Proc., Milwaukee, Wisconsin, USA, 2017
- [15] Wen, W., Huang, Y.: 'Research on operating mechanism for ultra-fast 40.5-kV vacuum switches', *IEEE Trans. Power Deliv.*, 2015, **30**, (6), pp. 2553–2560
- [16] Yuan, Z., He, J., Pan, Y., *et al.*: 'Research on ultra-fast vacuum mechanical switch driven by repulsive force actuator', *Rev. Sci. Instrum.*, 2016, **87**, (12), p. 125103
- [17] Peng, C., Song, X., Huang, A.Q., *et al.*: 'A medium-voltage hybrid DC circuit breaker – part II: ultrafast mechanical switch', *IEEE J. Emerging Sel. Top. Power Electron.*, 2017, **5**, (1), pp. 289–296
- [18] Li, W., Jeong, Y., Koh, C.S.: 'An adaptive equivalent circuit modeling method for the eddy current-driven electromechanical system', *IEEE Trans. Magn.*, 2010, **46**, (6), pp. 1859–1862
- [19] Fitzgerald, A.E., Kingsley, C., Umans, S.D.: *Electric machinery* (McGraw-Hill Higher Education, New York, NY, USA, 2003, 6th edn.)
- [20] Grover, F.W.: *Inductance calculations: working formulas and tables* (Instrument Society of America, USA, 1973)